Thermal Stability of Stearic Acid−Barium Stearate Langmuir−Blodgett Monolayers on Plasma-Oxidized Silicon Substrate Probed by Atomic Force Microscopy

C. Consalvo, S. Panebianco, B. Pignataro, G. Compagnini, and O. Puglisi*

Dipartimento di Scienze Chimiche, Università degli Studi di Catania, V.le A. Doria 6, 95125 Catania, Italy

Received: January 19, 1999; In Final Form: March 18, 1999

Mixed stearic acid−barium stearate Langmuir−Blodgett (LB) monolayers have been deposited on oxygen plasma oxidized silicon substrate. Atomic force microscope (AFM) has been used in order to obtain quantitative information about the coverage of the substrate after annealing at temperatures ranging from room temperature to 120 °C. These measurements allowed us to measure the rate constant K of the desorption process. Data showed that at low temperatures the formation of new holes (nucleation) and hole broadening (growth) have comparable rates, while at higher temperature nucleation has a catastrophic effect on the coverage. These observations suggest that different mechanisms are in action at temperatures above and below 55 °C, the hydration layer present between substrate and organic film probably playing a role in both mechanisms. Data are discussed in terms of both activated state theory and dynamical model.

Introduction

It is well-known that Langmuir−Blodgett (LB) films are very often not homogeneous and are degraded by aging and heating.[1] In the case of fatty acids it was found that LB films are stabilized by heavy divalent ions such as Zn, Ba, Cd, and so on.[2] However, considering the stability of these films, one must remember that both amphifilic moiety and substrate surface play important roles. In particular the substrate surface (silicon, mica, gold, etc.) is strongly dependent upon its preparation as well as subphase conditions.[1,3,4] With reference to LB films deposited from air−water interfaces or, in general onto hydrophilic substrates, there is the possibility to have water layers between substrate and LB film[5] that stabilize the system. On the other hand the thermal stability of the LB films play an important role in many of the possible applications such as nonlinear optics, molecular electronics, biosensors, and so on.[6,7] In these applications the knowledge of the thermal behavior, as well as of the factors that affect thermal stability is extremely useful.

The present work reports a kinetic study of thermal desorption of LB films of stearic acid/barium stearate deposited on oxygen plasma treated silicon surface. Atomic force microscopy (AFM) technique has been exploited in order to determine the surface coverage showing that desorption can take place following two different mechanisms depending on the temperature range considered. In particular the data show that at low temperature formation of new holes (nucleation) and hole broadening (growth) have comparable rate, while at higher temperature nucleation prevails and a catastrophic desorption is observed. In this last temperature range the rate-determining step has a temperature dependence in which the relevant energetic term is very close to the vaporization enthalpy of liquid water. The possible meaning of this temperature dependence is discussed in terms of activation state theory[8] and in terms of the dynamical model.[9]

Experimental Section

Stearic acid was obtained from Sigma (purity > 99%) and used without further purification. The monolayers were prepared in a trough (KSV 5000) by the LB vertical dipping technique. Stearic acid was dissolved in chloroform (0.6 mg/mL) and spread by a microsyringe (30 μL) on a subphase consisting of Millipore filtered water (resistivity about 18 MΩ) with $\cong 10^{-4}$ M $BaCl_2$ (pH = 6.8 ± 0.2). In these conditions a film containing a 2/1 mixture of stearic acid−barium stearate is formed.[10] The substrates were strips about 0.5 mm thick of monocrystalline silicon (1 cm × 2 cm) treated in a March barrel plasmod by an oxygen plasma (pressure = 1 mbar, power = 75 W, time = 3 min) to obtain a clean, homogeneous, and hydrophilic surface. The water contact angle, measured with a Kernco instrument, was $\theta \approx 5°$. Transfer was performed at a target pressure of 28 mN/m, a dipping speed of 5 mm/min, and a temperature of 20 °C in a thermostatic bath. Transfer ratios were approximately unity. Room-temperature experiments (ageing) were carried out in air at 21 ± 1 °C for a period ranging from 1 to 165 days. The average relative humidity in the laboratory was 42% ± 7%. Thermal treatments (annealing) were performed in air in a opened oven whose temperature, monitored by a thermocouple placed nearby the sample, was ranging from 40 to 120 °C. Annealing times ranged from 5 min to 24 h, the samples being heated from the silicon substrate side.

AFM measurements were performed in air at room temperature using a Digital Instruments nanoscope, model IIIa. Commercial silicon nitride, pyramidal tips (type NP Digital, internal angle of 70°, curvature radius of 20−50 nm) were used, whose chemical composition has already been investigated by XPS analysis.[11] These experiments were performed with cantilevers of nominal spring constant of 0.12 N/m. The AFM images are obtained in the constant force (height) mode with a nominal total force of about 10 nN in a slightly attractive regime. The scan rate ranged from 2 to 4 Hz. Slight damage of the sample induced by the probe has been observed only after several scans (typically 4) on the same region, consisting in the formation of new holes about 20−30 nm in size or in a broadening of preexisting ones. Evaluation of the covered surface ratio (σ) was performed by plotting the percentage of pixels (Hist %) versus the depth position. Typical distribution plots are reported in the upper part of Figure 1. These plots

10.1021/jp990213e CCC: $18.00
Published on Web 06/03/1999

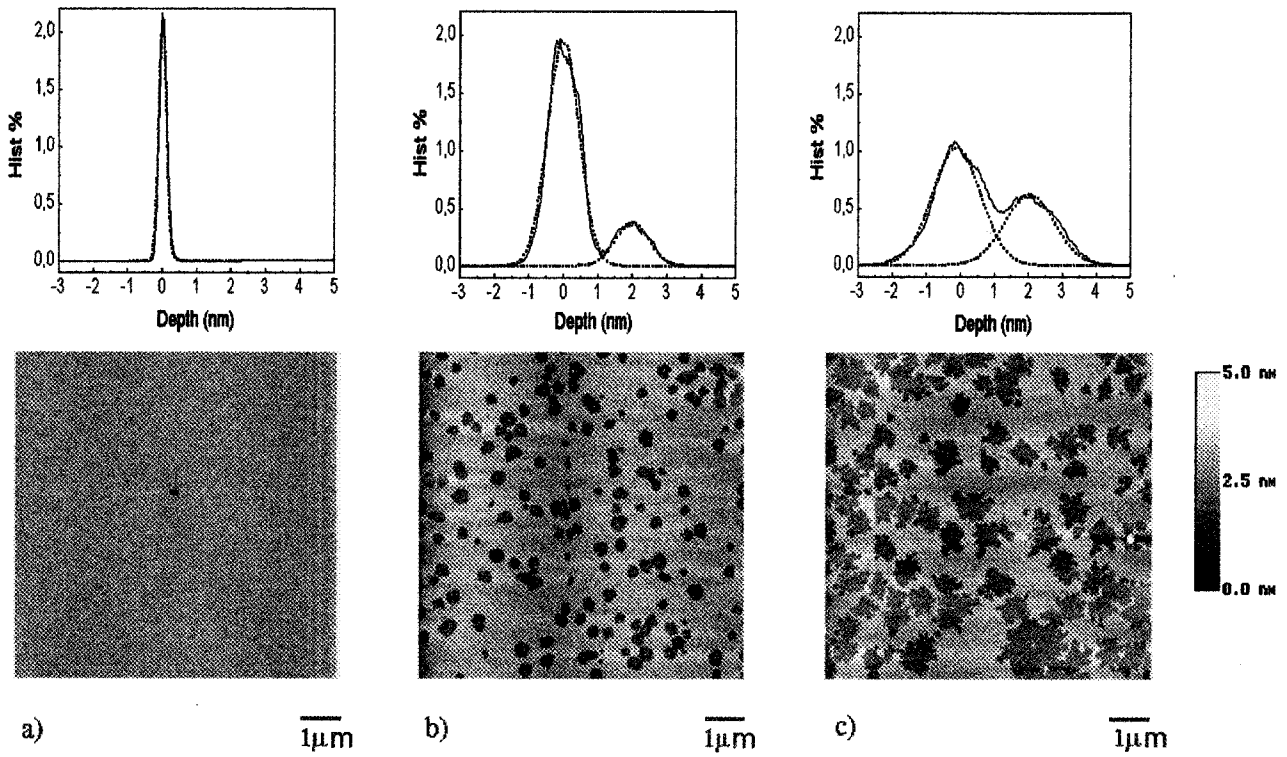

Figure 1. 10 μm × 10 μm 2D AFM images taken in contact mode on monolayers aged at room temperature: (a) freshly prepared barium stearate−stearic acid LB film, (b) 60 days aged sample, and (c) 130 days aged sample. The vertical bar on the right of the images shows the *z* color scale. Above each image the corresponding depth distribution plot is reported (see the Experimental Section). Each peak is fitted by Gaussian curves (dotted lines).

were derived from 10 μm × 10 μm 2D AFM images previously processed by subtracting from each scan line a third-order least squares calculated fit. This process removes the *z* offset between scan lines and the tilt and bow in each line. The distribution peaks were deconvoluted by Gaussian curves. The finite widths of the peaks are due to the slope at the edges of holes as well as an artificial slope introduced by tip convolution at the steps. Another contribution to the widths comes from an overall artificial curvature of the entire image due to the non linearity of the piezoelectric scanner.[12] Average values of film thickness reported in the discussion are calculated by section analysis performed on unprocessed images, collecting the depth of about 10 holes from several images for each sample.

Results

Room-Temperature (Aging) Effects. The sequence of Figure 1a−c shows the evolution of a sample during the aging process for 130 days at room temperature. The lower part of the figure refers to 2D AFM images while the upper part reports the corresponding depth distributions. It is to note that moving along the *x* axis from left to right of these distributions we find pixels corresponding to deeper surface points. Points at the top of the film are arbitrarily centered at zero depth. The second peak in Figure 1b and c corresponds to points lying on the substrate. The area of the first peak with respect to the total area of the peaks gives the value of σ. In Figure 1a it is reported a 10 μm × 10 μm image of a freshly prepared monolayer. Dark areas on the image correspond to holes on the film surface, while the lighter areas represent the film itself. The sample consists of a uniform, flat (roughness measured as root mean square of the *z*-height values (RMS) = 0.9 ± 0.2 Å) and defect free surface whose covered surface ratio is $\sigma = 1$. It is common to detect a hole near the center of the image (see Figure 1a), this being due to the fact that the engagement of the AFM tip with the surface involves much larger forces than those used for imaging. However, when one examines aged samples those central holes are absent, showing that aged monolayers are much more stable to the AFM tip damaging than the fresh ones. After a few days holes due to aging, about 40−60 nm in diameter, start to be observed even if their number does not affect significantly the value of σ. AFM images of those samples are not reported here. In Figure 1b it is reported the image of a 60 days aged monolayer. The corresponding value of σ is 0.80 ± 0.01. This image shows the presence of almost circular shaped holes, with diameters ranging from 150 to 500 nm. It is also possible to see that a process of coalescence of holes has begun. Figure 1c shows the surface of a 130 days aged monolayer. For this sample we measured a value of $\sigma = 0.63 \pm 0.01$. The AFM image shows that the surface coverage is rather inhomogeneous and rich of indented and irregular holes. Due to their shape, diameters of such holes are hard to estimate, but they approximately span from 300 nm to 1 μm. By counting the total number of holes in 10 μm × 10 μm AFM images, we note that for all samples there is a period of about 20 days in which nucleation is very fast (see Figure 2), while growth is a continuous process with a more or less constant rate along the time of observation. In the period between 20 and about 150 days from preparation, hole growth is the main process while the nucleation of new holes is negligible. In this period the total number of holes decreases due to coalescence. The two-dimensional Fast Fourier Transform (FFT) performed on these images is featureless, demonstrating that the hole edges do not have any well-defined absolute orientation.[12] The height values at the edges remain almost constant for each sample during aging, but on going from one sample to another, one observes a spread of values ranging from 14 to 25 Å, with a typical std deviation of about 2 Å. This spreading is probably due to different tilt of molecules with respect to the surface. However,

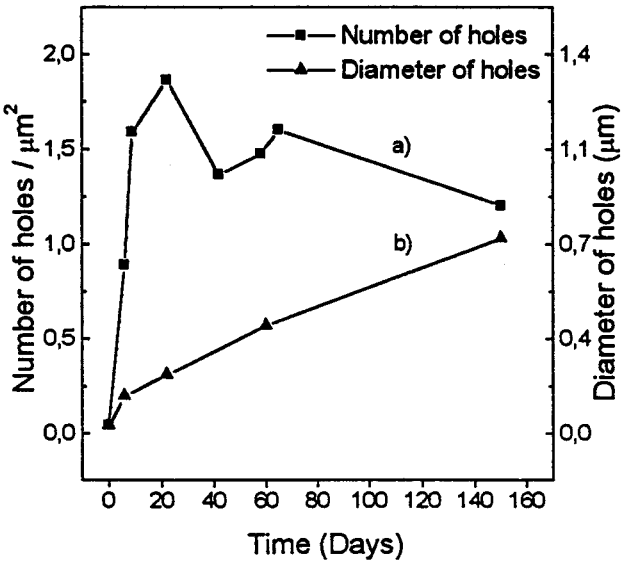

Figure 2. Plot of the number of holes (line a) and of their diameters (line b) versus aging time at room temperature. The lines are drawn to guide the eye.

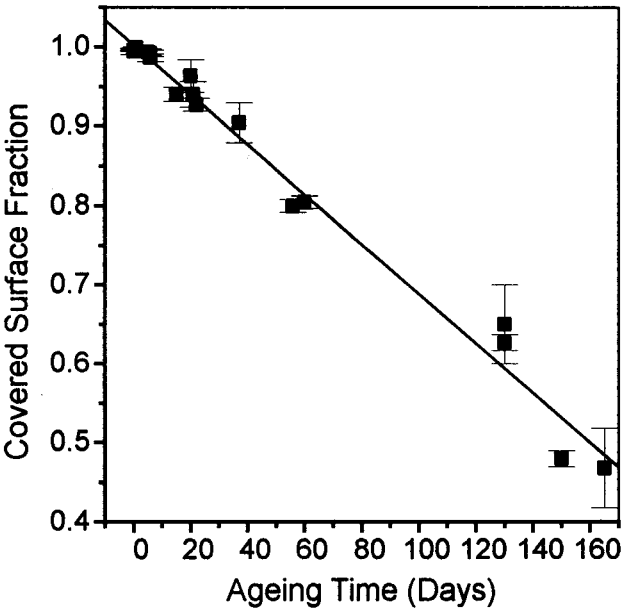

Figure 3. Plot of covered surface fraction (σ) versus aging time. The points represent mean values. Points are fitted by a straight line, i.e., a zeroth-order kinetic is assumed (see text).

height values are not significantly affected by aging and therefore they will not be taken in consideration in the following.

In a previous work on these systems[11] it was demonstrated that the desorption of molecules due to aging leaves a LB-free substrate surface. Therefore, since we do not observe formation of multilayers, nucleation and growth of holes should be due to desorption of molecules from the substrate.

In Figure 3 we report a plot of σ vs aging time. Values of σ have been monitored for a period of 165 days, and they range from 1 (for freshly prepared samples) to about 0.47 ± 0.05 (for 165 days aged samples). It is possible to make a linear fit of the data, and this would imply a zero order for the kinetic law of desorption at ambient temperature

$$-d\sigma/dt = K$$

where K is 3.8×10^{-8} s $^{-1}$.

However, in our case the rate of the process is too slow to be able to discriminate between exponential and linear decrease of σ in the time range we monitored. Thus one can also assume a first-order kinetic for the process,

$$-d\sigma/dt = K\sigma$$

where K is 4.0×10^{-8} s $^{-1}$.

The quality of the fit to the data (χ^2) using first or zeroth-order dependence is quite similar and does not allow us to distinguish between the two laws on the basis of quantitative considerations. However, in the assumption of zeroth order we might predict that the disappearance of the monolayer would be complete by about 300 days. On the contrary, samples aged for more than 300 days show again the presence of LB film. Although these samples do not allow reliable quantitative measurement of σ, due to the random distribution of the remaining LB film, the fact itself that LB film is again present allows us to discard the hypothesis of zeroth order kinetics.

Thermal Treatment Effects. In Figure 4a it is reported a 2D 10 μm $\times$ 10 μm AFM image of a stearic acid barium stearate monolayer annealed in air at 50 °C for 20 min ($\sigma = 0.65$). AFM images are taken after quenching the film in air at room temperature. We can see that the thermal treatment gives rise to formation of holes having, in the example of Figure 4a, a shape of drains (or worms) whose length ranges from 0.2 to 2 μm. Section analysis has been performed on AFM images, showing the presence of a holed terrace having the same height of the pristine sample. This demonstrates that in these conditions the process involves desorption of molecules with formation of defects (holes), leaving the system in a monolayer arrangement. Figure 4b and c report 2D 10 μm $\times$ 10 μm images of samples annealed in air for 20 min at 60 °C ($\sigma = 0.39$) and 80 °C ($\sigma = 0.27$), respectively. It is possible to see that at temperatures above 60 °C the thermal induced desorption leads to a surface with homogeneously distributed LB islands. Moreover, on going to higher temperatures (at constant time) [or to longer times (at constant temperature), not shown in figure], one observes a decrease of the size of the LB film features. In particular LB films show features having mean size going from 800 to 1000 nm at 50 °C, from 70 to 200 nm at 60 °C, and from 40 to 100 nm at 80 °C. By annealing at even higher temperatures we observe the formation of droplets (typical conditions used to observe this phenomenon are 12 min at 120 °C). This result is similar to the finding of Tippmann-Krayer et al.[13] who showed the formation of droplets in LB multilayer films of cadmium arachidate deposited on oxidized silicon wafers due to heating at temperatures above 150 °C. Section analysis performed across the droplets allowed us to measure their heights, which range from 4 to 6 nm, and to observe that their structure is that of multilayers spaced one another of about 20 Å, which is close to the height of one barium stearate-stearic acid monolayer. Our observation is in contrast with the findings of ref 13 where it is reported that the droplets are structureless. This shows that at these temperatures desorption is accompanied for the studied samples by rearrangement and formation of multilayers. In Figure 5 we report a plot of ln(σ) vs annealing time with annealing temperatures ranging from 50 to 120 °C. It is evident the linear decrease of ln(σ) with time, with different rate for each temperature. Values of the rate constant K range from 5.49×10^{-3} (at 120 °C) to 3.50×10^{-4} s^{-1} (at 50 °C). As in the case of aging, thermal desorption is isotropic, as shown by FFT analysis (not reported here). It is important to notice that the time needed to reach the value of $\sigma = 0.5$ is about 10 min at 80 °C and about 15 min at

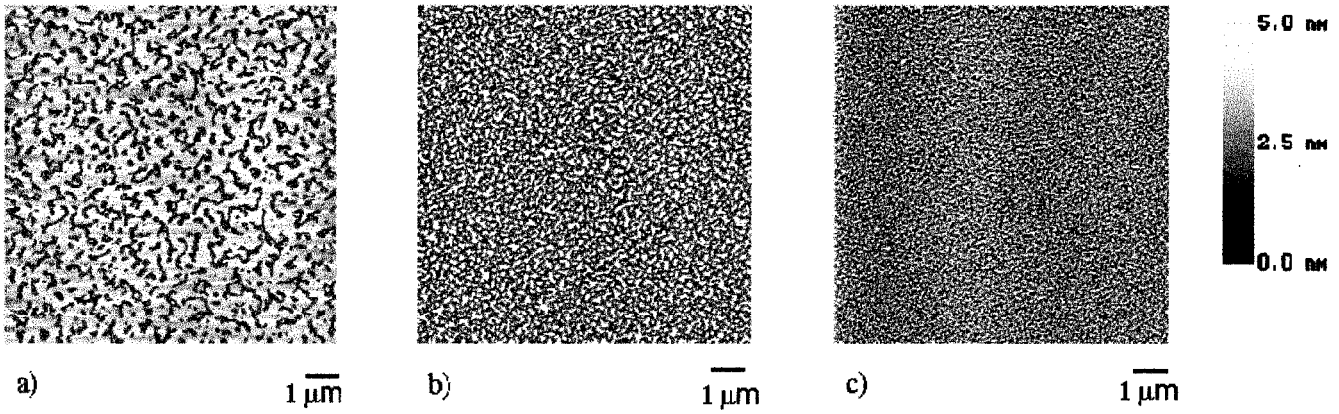

Figure 4. 10 μm × 10 μm 2D AFM images of samples thermally treated for 20 min: (a) sample treated at 50 °C showing worm like holes, (b) sample treated at 60 °C showing small LB islands 70−200 nm in size, and (c) sample treated at 80 °C showing smaller islands 40−100 nm in size. The order of magnitude of the number of molecules present in each island is about 2×10^4.

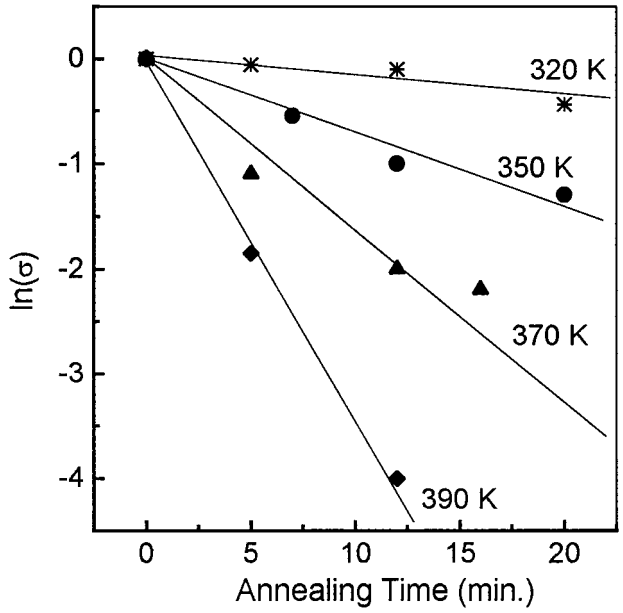

Figure 5. Plot of ln(σ) versus annealing time. The slopes of the lines give the rate constants reported in the plot of Figure 6.

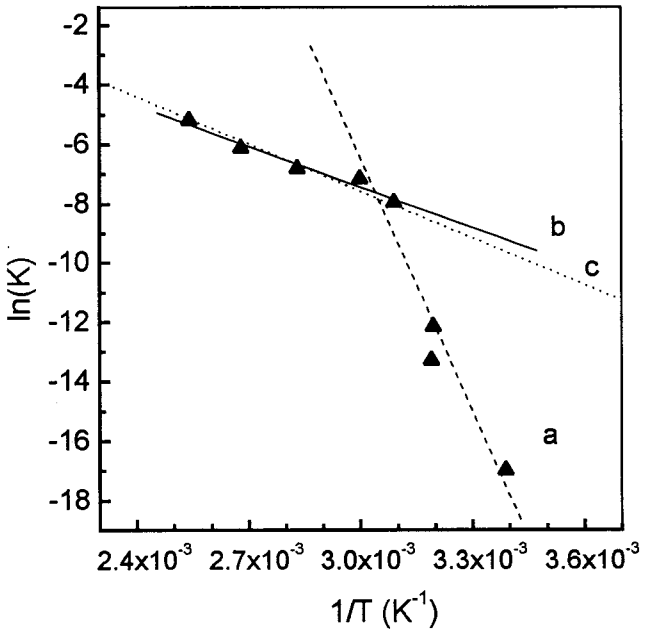

Figure 6. Dependence of ln(K) on 1/T. Line a is the best fit of the points obtained at low temperatures (from room temperature to 50 °C). Line b is the best fit of the points obtained at high temperature (from 50 to 120 °C). Line c is a curve with a slope equal to $-\Delta H_{ev}/k$ where ΔH_{ev} is the enthalpy of evaporation of liquid water at 60 °C. It is possible to see that line c fits well the experimental data.

60 °C, while about 150 days are needed at room temperature. We note also that samples treated at the higher temperatures have more homogeneous distribution of the characteristic features than the ones at lower temperatures. This is consistent with the fact that at low temperature nucleation and growth have a more or less comparable rate (see Figure 2), while at the higher temperatures one observes catastrophic hole nucleation (see Figure 4b and c). In these cases, growth is strongly limited by nucleation so that the process gives rise to holes with almost monodisperse size distribution. In particular, the large hole number and their crowding leads to a island-like distribution of the remaining LB film.

To fit the experimental data with a kinetic law, we note that a first-order kinetic of the type $-d\sigma/dt = K\sigma$ is the best one. This is at variance with the case at low temperature (see above) where both zero and first-order laws could fit the data, because at high temperature the process rate is so high that we explored the desorption till to coverage fraction close to zero and this allowed us to discard the hypothesis of a zero order kinetics.

As to the rate constant K we expect the usual Arrhenius-like temperature dependence

$$K = A \exp(-\Delta E^+/kT)$$

where ΔE^+ is the activation energy of the process, A the frequency factor, and k the Boltzmann constant. The related Arrhenius plot is shown in Figure 6.

In this plot the points match two different lines. Line b in Figure 6 fits values of ln(K) obtained by annealing at temperatures ranging between 50 and 120 °C. From the slope of the line we calculate an activation energy of 40 ± 4 kJ/mol and a frequency factor $A = 5 \times 10^2$ s^{-1}. Line a in Figure 6, characterized by a much steeper slope, fits values of ln(K) between room temperature and 50 °C. The corresponding activation energy is 230 ± 50 kJ/mol, and A assumes the value of 2×10^{34} s^{-1}.

Discussion

The observation of two distinct lines in the Arrhenius plot reported above is in agreement with AFM morphology, since on going from low to high-temperature ranges hole features are replaced by an island like situation. The sudden change in slope

of this diagram may be due to a some pretransitional disordering of the LB layer[14,15] occurring at a temperature lying between 50° and 60 °C. Surprisingly, the melting temperature of bulk stearic acid is reported close to this temperature, at 68 °C. Thus the change of the slope could be due to some structural disordering of the LB layer near to the bulk phase transition.

We must conclude that the phenomenon here reported is governed by two mechanisms with a transition temperature located somewhere between 50 and 60 °C.

The temperature dependence of the rate constant such as that experimentally observed here is normally explained using the concept of activated transition state. Moreover, for thermal desorption of LB films the activation energy value has been often assumed in the literature to take the meaning of binding energy of the species that desorb in the rate-determining step.[16,17] In our case this interpretation would imply that at low temperatures ($T \leq 55$ °C) the chemical species involved in the rate determining step has a high binding energy (230 ± 50 kJ/mol), while at high temperatures ($T > 55$ °C) the mechanism at work is one with a lower binding energy (40 ± 4 kJ/mol). The puzzling fact here is that the activation energy at low temperature is close to the sublimation energy of bulk stearic acid (175.5 kJ/mol), while the activation energy at high temperature is very close to the vaporization energy of liquid water at 60 °C. Of course these numerical coincidences cannot be used as analytical proofs that the species involved in the rate determining steps are stearic acid and water, at low and high-temperature respectively, but the fact is intriguing. According to the present Authors opinion, the most difficult thing to accept is that if one follows this interpretation one is forced to explain a monolayer behavior in terms of thermodynamic parameters of bulk phases.

Further difficulty arises examining the preexponential factor of the rate constant K:

$$K = A \exp(-\Delta E^{+}/kT)$$

In our case A assumes the value of 2×10^{34} s^{-1} at low temperature and the value of 5×10^{2} s^{-1} at high temperature. The difference of 32 orders of magnitude between the two preexponential factors is huge and, even if it could be explained in terms of different precursor models,[18] it remains, anyway, hard to accept.

Identical considerations have been made by other Authors in similar cases,[16] and in general, when one try to account for different activation energy values one must use preexponential factors that differ each other by unrealistically high factors. This is, probably, one of the most troublesome consequence of the practical use of activation energy concept.

In our case it seems more realistic (even if much less convenient from the computational point of view) to explain the above data in terms of dynamical model.[9,19] In other words we believe that the experimentally observed Arrhenius type temperature dependence of the LB desorption rate constant (i.e., the process is "activated") does not necessarily mean that we have a true activated transition state.

Criticism to the transition state concept is well-known. The most important for our purpose is that there is not any plausible proof that this activated state (if any) has a mean lifetime long enough to achieve thermodynamic equilibrium. Moreover, the number of molecules present in each LB island is of the order of about 2×10^{4} (see Figure 4c for example) and it seems unrealistic to adopt thermodynamic concepts for a so low number of molecules.

We note that, in the framework of the dynamical model, again, the temperature dependence is of the type

$$d(\ln K)/d(1/T) = -\Delta H/k$$

as in the activated state theory, but here the meaning of the energy term is not that of a "free-energy barrier", but of the minimum energy required for the species considered to achieve critical vibrational amplitude necessary for the diffusional jump (plus other energetic contributions related to the shell constituents).[9] In other words, we believe that the dynamical model would better account for the observed temperature dependence of the rate constant. More precisely, if we make the assumption that stearic acid and water are the relevant species for the rate-determining steps at low and high temperature, respectively, thus in the framework of the dynamical model the minimum energy required to achieve critical vibrational amplitude should numerically be very close to the sublimation energy of bulk stearic acid and to the vaporization energy of liquid water, at low and high temperatures, respectively. Confirming or disproving this hypothesis will be the task of future dynamical simulation of this system.

As to the difficulty related to the 32 orders of magnitude between the preexponential factors (see above), it is probably due to the fact that the true kinetics of the phenomenon is more complex than that we hypothesise. Probably many consecutive reactions take place in our case, giving rise to pseudo-first-order kinetics, so that the preexponential factors one obtains experimentally, really include other factors such as the concentrations of other species involved in the reaction.

In any case, a detailed model of this kinetics must take in consideration the most important conclusion drawn from the phenomenological model (see Figure 2), i.e., we are dealing with two mechanisms: hole nucleation and hole growth. In other words, the simple "one rate constant model" here sketched is not adequate to describe a complex phenomenon where nucleation and growth compete in determining the LB desorption. These two situations are quite different each other under both the point of view of the frequency factor and the relevant energetic term: (a) when nucleation prevails desorption takes place from a topologically "undisturbed" film where each molecule is surrounded by an ordered ensemble of partner molecules (b) in the hole growth regime the molecules lying at the border between covered and uncovered regions, the "hole boundary molecules", are surrounded by about one-half of partner molecules so that they might desorb at different rate.

Conclusion

This paper has shown that thermal desorption of stearic acid/Ba stearate LB monolayer film is governed by two mechanisms. In the first one, at $T \leq 55$ °C, nucleation and growth of the holes have comparable rate. In the second one, at $T > 55$ °C, hole nucleation is catastrophic and prevails on growth. The relevant energetic terms in the Arrhenius-like temperature dependence of the rate constants are surprisingly close to thermodynamical bulk values (sublimation energy of bulk stearic acid and vaporization energy of liquid water). Probably the coincidence is not random but it seems hard to explain a monolayer behavior in terms of (equilibrium) thermodynamical parameters of bulk phases. Probably the use of the dynamical model, in place of the activated state theory, will explain these energetic terms in a more realistic way.

The main problems left unresolved by this study and the corresponding subjects for future work are (a) to make a detailed

kinetic analysis of the phenomenon. To this end it will be important to consider that this is a complex system where chemical strong interactions between "hydrophilic" SiO_2 surface and stearic acid/Ba stearate mixture coexist with interactions less intense, yet important, such as those provided by the water layer. To this end it will be useful to extend the study at films deposited at pH where acid (pH6) or salt (pH>9) molecules only exist;[1] (b) to perform numerical simulations in the framework of a detailed dynamical model where all the above interactions can be taken in account; (c) to establish the true role of the water layer.

That water is important in stabilizing LB films[5] or supramolecular complexes[20] is already known, but the precise role in the system here studied remains to be established. However, we begin to have enough experimental evidence that the flux of water that evaporates from the LB film during thermal treatment is important in determining the overall rate of the phenomenon. To prove this we have repeated the experiments shown in Figure 6 (line b) with the only difference that the partial pressure of water in the ambient air was very high and close to the saturation value (order of magnitude about 100 Torr, while in the experiments of Figure 6 the partial water pressure in the ambient air was about 10 Torr). The very interesting result of these experiments[21] is that the rate of LB disappearance was reduced of about 1 order of magnitude. Therefore, we are forced to conclude that LB "drying" rate play an important role with respect to monolayer stability.

Acknowledgment. We acknowledge Consorzio Catania Ricerche for the hospitality in the lab and the technical support of its staff. CNR (Rome) and MURST are acknowledged for partial financial support. The authors thank Prof. A. Raudino for useful discussions.

References and Notes

(1) Schwartz, D. K. *Surf. Sci. Rep.* **1997**, 27, 241.
(2) Bloch, J. M.; Yun, W. *Phys. Rev. A* **1990**, 41 (2), 844.
(3) Kurnaz, M. L.; Schwartz, D. K. *J. Phys. Chem*. **1996**, 100, 11113.
(4) Schwartz, D. K.; Viswanathan, R.; Garnaes, J.; Zasadzinski, J. A. *J. Am. Chem. Soc*. **1993**, *115*, 7374.
(5) Viswanathan, R.; Schwartz, D. K.; Garnaes, J.; Zasadzinski, J. A. N. *Langmuir* **1992**, *8*, 1603.
(6) Zasadzinski, J. A. N.; Viswanathan, R.; Madsen, L.; Garnaes, J.; Schwartz, D. K. *Science* **1994**, *263*, 1726.
(7) Ulman, A. *An Introduction to Ultrathin Organic Films from Langmuir−Blodgett to Self-Assembly*; Academic: New York, 1991.
(8) Eyring, H. *J. Chem. Phys*. **1935**, 3, 107.
(9) Rice, S. A. *Phys. Rev*. **1958**, *112*, 804.
(10) Vogel, C.; Corset, J.; Billoudett, F.; Vincent, M.; Dupeyrat, M. *J. Chim. Phys*. **1980**, *77*, 947.
(11) Pignataro, B.; Consalvo, C.; Compagnini, G.; Licciardello, A. *Chem. Phys. Lett.* **1999**, *299*, 430.
(12) Schwartz, D. K.; Viswanathan, R.; Zasadzinski, J. A. N. *J. Phys. Chem.* **1992**, 96, 10444.
(13) Tippmann-Krayer, P.; Meisel, W.; Möhwald, H. *Adv. Mater*. **1990**, *2*, 589.
(14) Riegler, J. E. *J. Phys. Chem.* **1989**, *93*, 6475.
(15) Rothberg, L.; Higashi, G. S.; Allara, D. L.; Garoff, S. *Chem. Phys. Lett.* **1987**, 133, 67.
(16) Laxhuber, L. A.; Rothenhäusler, B.; Schneider, G.; Möhwald, H. *Appl. Phys. A* **1986**, *39*, 173.
(17) Tippmann-Krayer, P.; Möhwald, H. *J. Phys. Chem.* **1992**, *96*, 5220.
(18) Gorte, R.; Schmidt, L. D. *Surf. Sci.* **1978**, 76, 559.
(19) Schmalzried, H. *Solid State Reactions*; Verlag Chemie: Weinheim, 1981; p 79.
(20) Barbour, L. J.; Orr, G. W.; Atwood, J. L. *Nature* **1998**, *393*, 671.
(21) Puglisi, O. et al., to be published.